Human-induced changes in the distribution of rainfall

Aaron E. Putnam[1,2]* and Wallace S. Broecker[2]

A likely consequence of global warming will be the redistribution of Earth's rain belts, affecting water availability for many of Earth's inhabitants. We consider three ways in which planetary warming might influence the global distribution of precipitation. The first possibility is that rainfall in the tropics will increase and that the subtropics and mid-latitudes will become more arid. A second possibility is that Earth's thermal equator, around which the planet's rain belts and dry zones are organized, will migrate northward. This northward shift will be a consequence of the Northern Hemisphere, with its large continental area, warming faster than the Southern Hemisphere, with its large oceanic area. A third possibility is that both of these scenarios will play out simultaneously. We review paleoclimate evidence suggesting that (i) the middle latitudes were wetter during the last glacial maximum, (ii) a northward shift of the thermal equator attended the abrupt Bølling-Allerød climatic transition ~14.6 thousand years ago, and (iii) a southward shift occurred during the more recent Little Ice Age. We also inspect trends in seasonal surface heating between the hemispheres over the past several decades. From these clues, we predict that there will be a seasonally dependent response in rainfall patterns to global warming. During boreal summer, in which the rate of recent warming has been relatively uniform between the hemispheres, wet areas will get wetter and dry regions will become drier. During boreal winter, rain belts and drylands will expand northward in response to differential heating between the hemispheres.

INTRODUCTION

High on the list of likely consequences of human-induced climate change is the redistribution of rainfall. Although water for domestic use can be produced affordably by desalination, that required for agriculture cannot. Rather, it must be supplied by natural sources, such as direct rainfall and irrigation from surface and underground reservoirs. Despite efforts to improve management of freshwater resources, increases in human population, meat eating, and industrial water usage are already creating shortages. The impact of anthropogenic changes will further complicate this already serious situation. Here, we discuss one of these complications, namely, the redistribution of water resulting from a warming planet.

On the basis of simulations carried out in atmosphere-ocean models, two hypothetical global changes in the pattern of rainfall stand out. One hypothesis suggests that, as the world warms, rainfall will become increasingly focused on the tropics (Fig. 1) (1). Although, by this hypothesis, net global precipitation will increase, the precipitation increase will be dominantly registered in the tropical rain band, and the subtropics and middle latitudes will become drier. The other hypothesis is that the world's tropical and mid-latitude rain belts are tied to the latitude of the thermal equator. Hence, as CO_2 has and likely will continue to heat the Northern Hemisphere faster than the Southern Hemisphere (Fig. 2), the world's rain belts [that is, the intertropical convergence zone (ITCZ) and mid-latitude storm tracks] may shift to the north (2–4). This happens annually (see Fig. 3). The thermal equator shifts to the north during boreal summer and to the south during boreal winter. The record for the past 30,000 years (30 ky) kept in the shorelines of closed-basin lakes supports both of these model-based predictions. During peak glacial time [the last glacial maximum (LGM); 26 to 18 ky ago (5)], the extratropics were wetter. During the period of deglaciation (18 to 11 ky ago), the world's rainfall belts jumped back and forth following rapid hemispheric switches in the extent of polar sea-ice cover. Here, we make a

case that the paleoclimate record can be used as a guide for how the planet's hydrological system might evolve as global temperatures rise in response to the injection of fossil CO_2 into the atmosphere. Just as with the case of the last glacial termination, we envision a hybrid response that involves not only tropical focusing of rainfall with drying of the extratropics (specifically the subtropics and middle latitudes) but also a concomitant shift of the tropical rain belts and mid-latitude storm tracks in lockstep with the northward march of the thermal equator—at least during the global warming transient.

THE IMPACT OF GLOBAL TEMPERATURE

Conditions at the peak of the last ice age afford a means by which the Held and Soden (1) "wet-get-wetter, dry-get-drier" hypothesis can be tested using the paleoclimate record. For example, if a warmer world is expected to produce increased tropical and decreased subtropical/mid-latitude rainfall, then the converse situation that a colder world would support drier tropics and wetter extratropics should hold. The most convincing evidence that global cooling reduces the extent to which rainfall is focused on the tropics comes from closed-basin lakes located in the 35° to 40° latitudinal belts (Fig. 4). Because these lakes have no outlets, the water supplied by river inflow is lost by evaporation rather than outflow. This being the case, the greater the input of river water, the larger the lakes become. Hence, elevated shorelines record past times of greater precipitation. As shown in Fig. 3, closed-basin lakes in western North America's drylands (6–8), in the Middle East (9), and in South America's Patagonian drylands (10) were all larger than today during the time when mountain glaciers stood at their maximum extent (11–13). The ages of the corresponding glacial maximum shorelines have been established by a combination of radiocarbon and radiothorium dating.

Because these lakes were 3 to 10 times larger than now during peak glacial time, it is clear that the glacial expansion cannot be explained by enhanced precipitation alone. Rather, it must be coupled with a large amplification. It turns out that the percentage change in lake areas is much larger than can be accounted for by precipitation. The reason for this relates to what hydrologists refer to as the Budyko effect (14):

[1]School of Earth and Climate Sciences and Climate Change Institute, 224 Bryand Global Sciences Center, University of Maine, Orono, ME 04469, USA. [2]Lamont-Doherty Earth Observatory of Columbia University, 61 Route 9W/PO Box 1000, Palisades, NY 10964, USA.
*Corresponding author. Email: aaron.putnam@maine.edu

Precipitation response to global warming
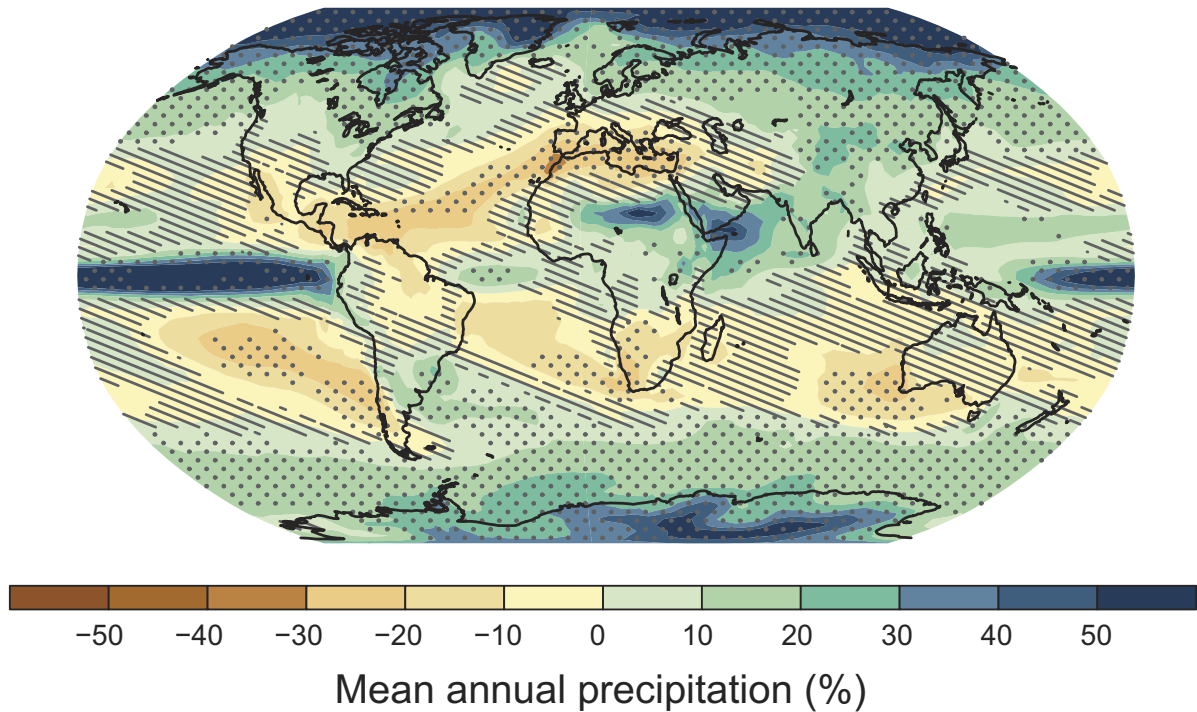
Fig. 1. Dependence of tropical focusing of rainfall on Earth temperature as determined using an ensemble of general circulation models. Map depicts regions that will get wetter (green and blue shades) and drier (brown shades) as the planet warms. The figure is reproduced with permissions from Figure SPM.7 in the Intergovernmental Panel on Climate Change AR5 Report [Summary for Policy Makers, pg. 12 (*95*)] and is based on the approach of Held and Soden (*1*). Data are from the ensemble average of the Coupled Model Intercomparison Project Phase 5 (CMIP5)/Intergovernmental Panel on Climate Change (IPCC) RCP 8.5 modeling results (*95*).

Temperature trend (°C)
(over period from 1951 to 2015 CE)
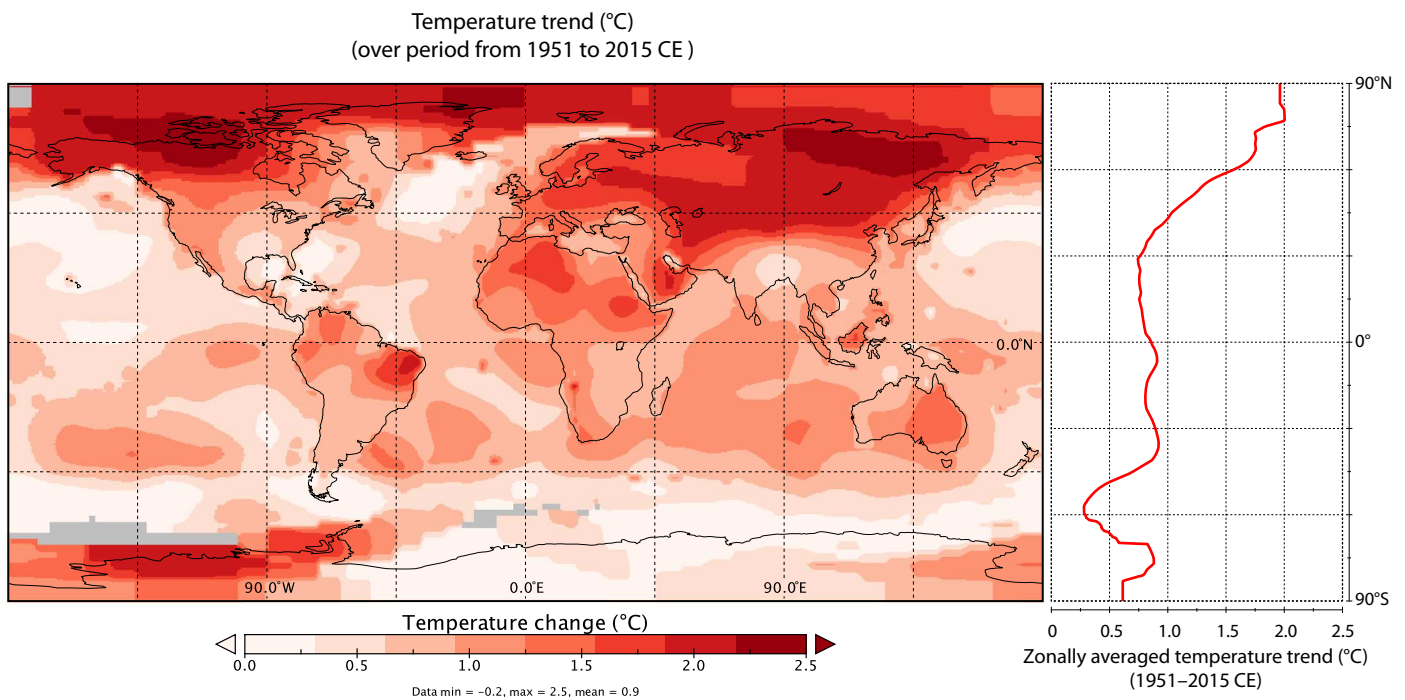
Fig. 2. Globally distributed temperature trends for the period CE 1951 to CE 2015. Left: Global map of temperature trends calculated for the period CE 1951 to CE 2015. Right: Zonally averaged temperature trends. The northern middle and high latitudes have warmed roughly twice as much as corresponding southern latitudes over the past half-century or so. Plots are based on the GISTEMP (Goddard Institute for Space Studies Surface Temperature Analysis) Reanalysis data set (*96, 97*).
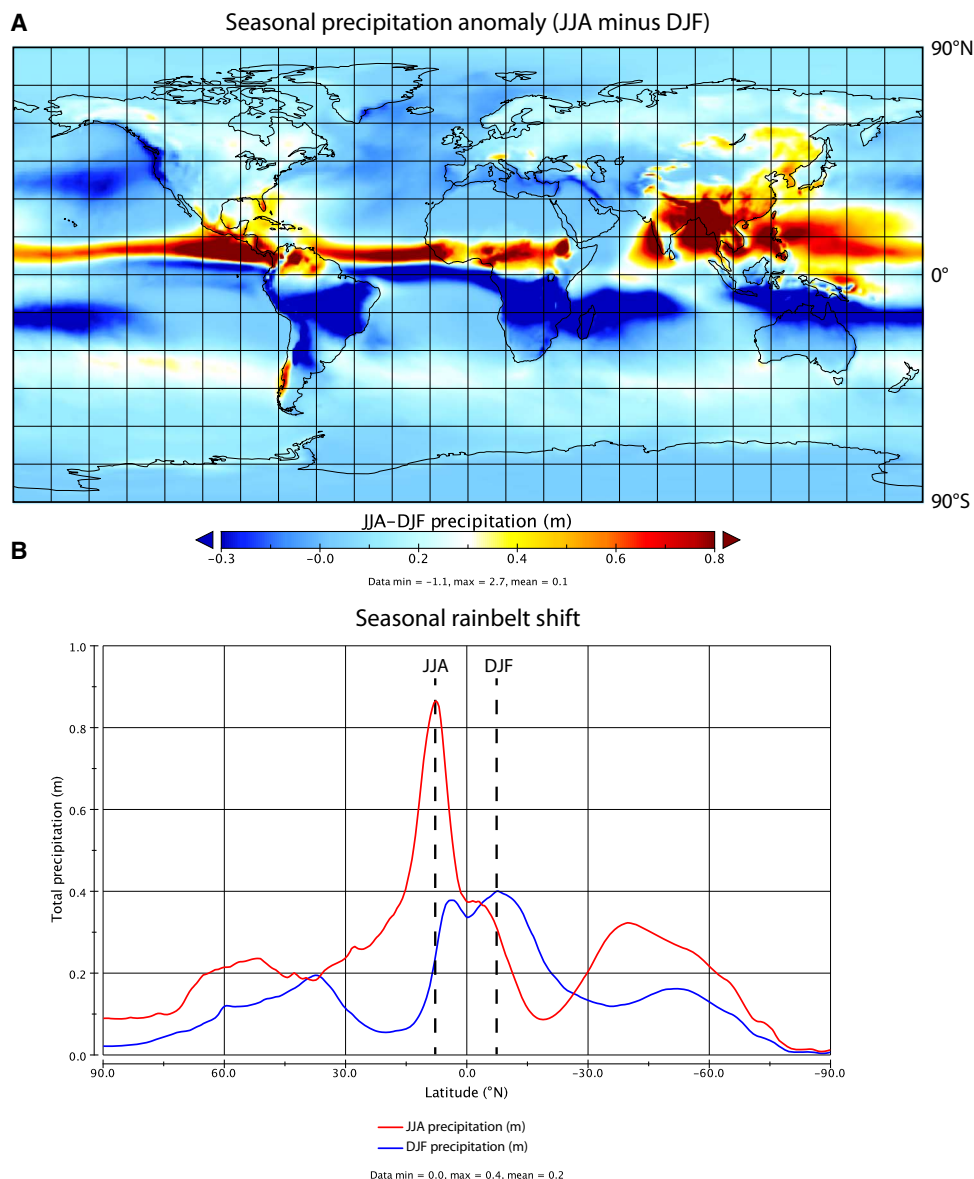
Fig. 3. Seasonal shift of Earth's rain belts. (**A**) Map illustrates the global seasonal precipitation anomaly [June-July-August (JJA) precipitation minus December-January-February (DJF) precipitation]. Red shades depict the position of the rain belts in the boreal summer, and blue shades indicate the position in the austral summer. (**B**) Plot of zonally averaged precipitation for JJA (red curve) and DJF (blue curve). Note the southward shift of the precipitation maximum that occurs between boreal summer and winter. Plots are based on data averaged over the period CE 1979 to CE 2015 from NASA Modern Era Retrospective Analysis for Research and Applications (MERRA) (*98*).

The greater the precipitation, the greater the fraction of water that runs off. For each 10% increase in rainfall, there is, on average, a 30% increase in runoff. Therefore, for example, a twofold increase in rainfall could explain a sixfold increase in lake area. Koster *et al.* (*15*) picked up on this and compiled precipitation and runoff data for 2000 drainage basins. While confirming that, on the average, there is a threefold amplification, they showed that the situation for individual drainage basins varies widely around this average. The magnitude of the amplification depends on topography, snowfall, plant cover, seasonality, etc. This amplification has widespread future importance because it applies to man-made reservoirs used to store water for agricultural use (*16*).

Other factors also influence the area of closed-basin lakes. One is that the rate of evaporation from a lake depends on temperature. Another is that part of the water vapor produced by lake evaporation rains back out

before escaping the bounds of the lake's drainage basin (*17*). Furthermore, although closed to overflow, water may leak into fracture zones beneath the lake. However, despite these complications, the message is clear that in the colder ice-age world, precipitation in the 30° to 40° midlatitude dryland band was larger than today. This suggests that, as fossil fuel CO_2 warms the world, these areas will become drier (*1, 8, 11*).

THE IMPACT OF DISPLACEMENTS OF THE THERMAL EQUATOR
Responding to abrupt changes in the extent of winter sea-ice cover in the northern Atlantic during the period of deglaciation, the planet's thermal equator jumped north and south (*18, 19*). During times of enhanced northern sea-ice cover, it moved to the south. During times of reduced sea-ice cover, the thermal equator moved to the north. The largest of
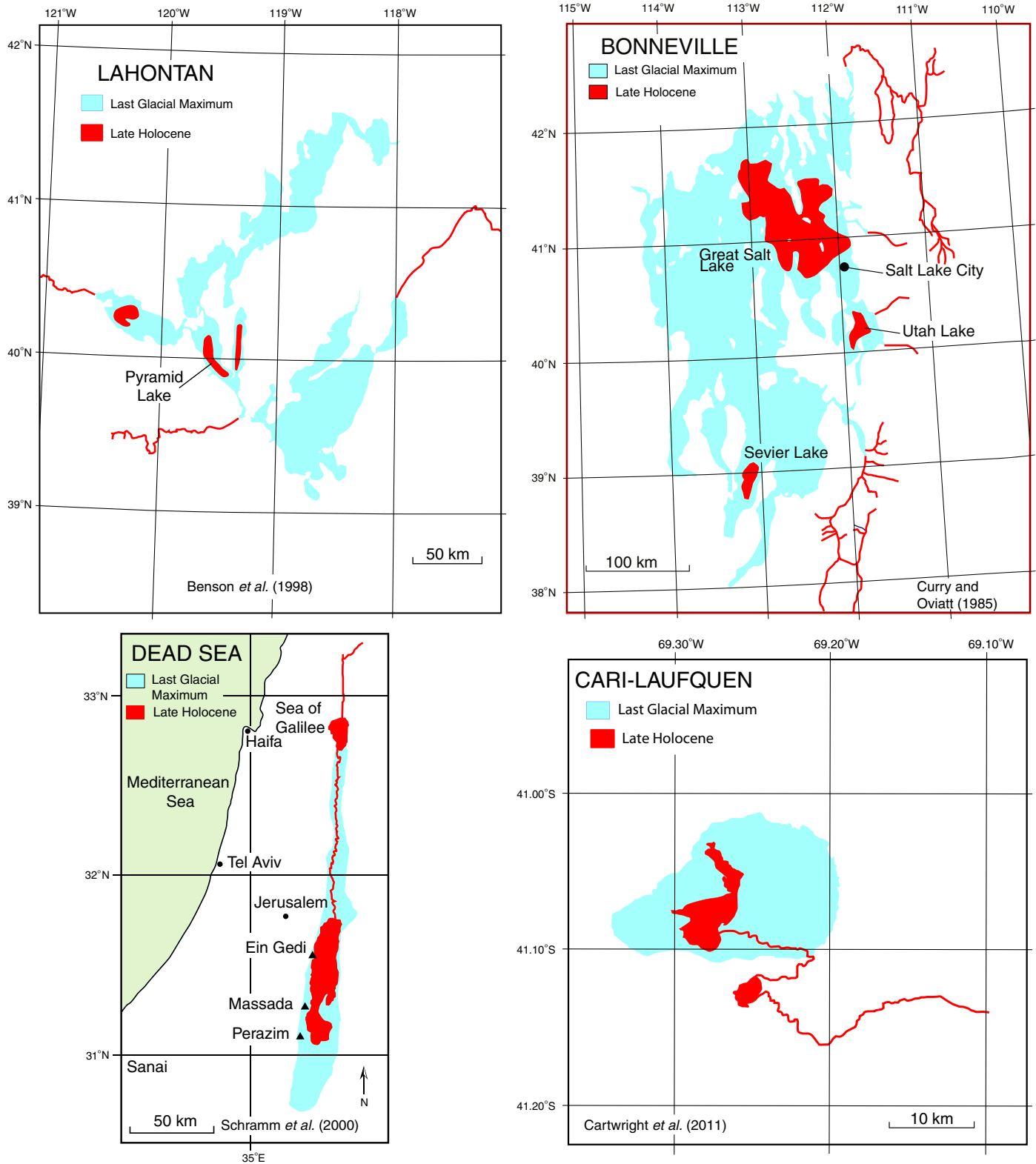
Fig. 4. Composite showing LGM (blue) and Late Holocene (red) extents of Lakes Lahontan, Lake Bonneville, the Dead Sea, and Lago Cari-Laufquen. These four closed-basin lakes (two in the Great Basin of the western United States, one in Israel-Jordan, and one in Argentina's Patagonian drylands) were much larger during the LGM compared with the late Holocene (red) (46). This difference reflects generally wetter conditions in the subtropics and middle latitudes during planetary cold episodes, partially at the expense of the drier tropics (1).

these northward jumps occurred 14.6 ky ago. We will focus on this event not only because we have a more complete record of its global impacts but also because the ongoing global warming will produce a shift of the thermal equator (Fig. 5), and possibly Earth's hydroclimate, in the same direction. One reason is that the Northern Hemisphere has twice as much land as the Southern Hemisphere and thus can heat up faster. Another reason is that the deep mixing in the Southern Ocean creates a "thermostat," holding back warming (20). Thus, the Northern Hemisphere can heat up more rapidly than the Southern Hemisphere, thereby steepening the interhemispheric thermal gradient and forcing a northward shift of the thermal equator.

The record preserved in ice tells us that Greenland's temperature underwent an abrupt 10°C mean annual warming 14.6 ky ago (21), marking the onset of the Bølling-Allerød interval. Most of this warming is thought to have occurred during winters (22, 23). The pre–14.6-ky cold, dubbed the "Mystery Interval" (24) or "Heinrich Stadial 1" (25), was the result of the presence of vast winter sea-ice cover over the density-stratified northern Atlantic (22, 26–28). Consequently, no ocean heat could reach the surface, and much of the incoming sunlight was reflected back to space. This being the case, winters in western Europe and Scandinavia would have been much like those in Siberia today (22, 29). During the Mystery Interval, the combination of more sea ice in the north and less in the south pushed the thermal equator to the south. Then, 14.6 ky ago, the situation abruptly switched. A rejuvenation of deepwater formation in the northern Atlantic (27) eliminated winter sea ice there. Although less certain, the extent of sea-ice cover in the Southern Ocean appears to have been antiphased with that in the northern Atlantic. The record kept by diatom accumulation in Southern Ocean sediments suggests that around 14.6 ky ago, the austral westerlies shifted equatorward, upwelling subsided, and sea-ice cover around the Antarctic continent presumably expanded (30, 31). This switch pushed the thermal equator back to
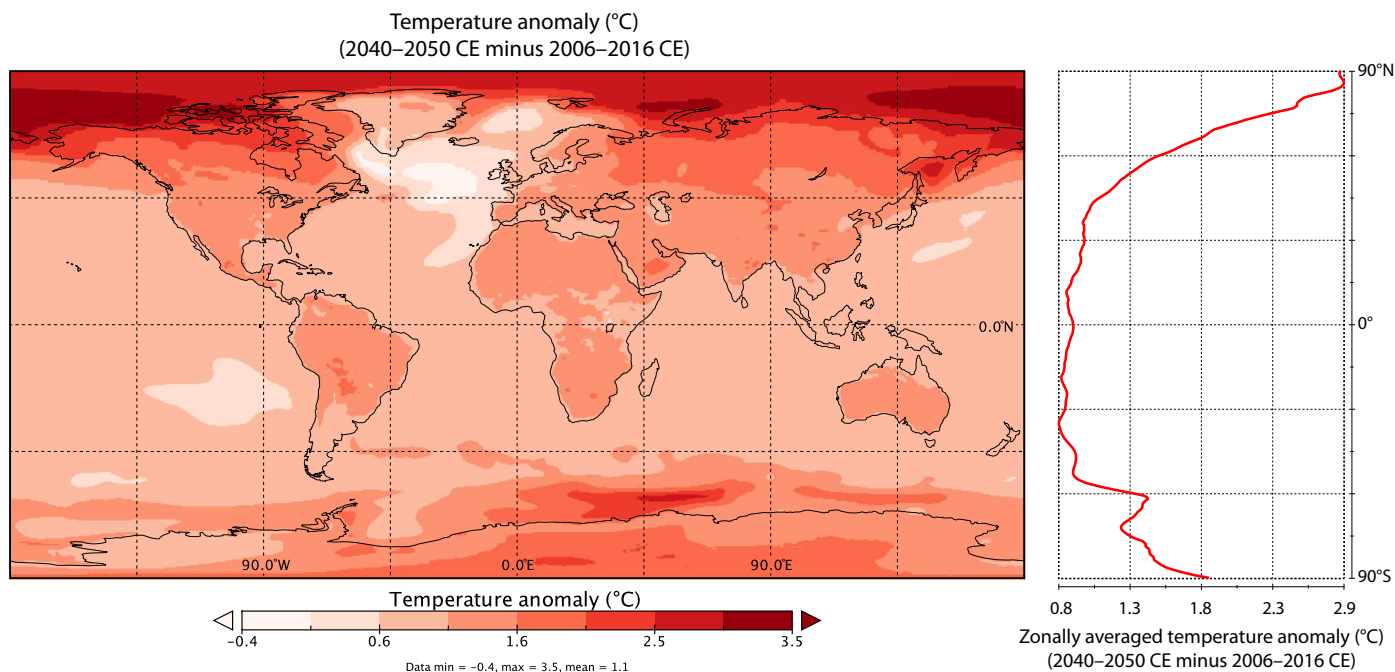
the north (19, 32, 33). Because the latitude of Earth's rain belts and dry zones are, at least in part, tied to the position of the thermal equator, this climatic change caused widespread changes in precipitation.

The expression of this hydrologic reorganization is featured in records obtained from continental margin sediments, stalagmite calcite, closed-basin lake shorelines, leaf waxes, and ice cores, to name a few. Here, we review a selection of pertinent paleoclimate records from tropical and extratropical regions that document the global hydrological response to the northward jump of the thermal equator that took place 14.6 ky ago.

Amazonia

Records of continental runoff and stalagmites from areas surrounding the Amazon afford insight into the behavior of the tropical rain belt over South America during the abrupt change 14.6 ky ago. Continental margin sediments consist primarily of soil detritus supplied by rivers and $CaCO_3$ produced by marine plankton. The detritus has a dark color, and the $CaCO_3$ has a light color. Scans of sediment color provide a qualitative measure of the ratio of relative contributions of these two components. The same information can be obtained by measuring, for example, the ratios of calcium to iron or calcium to titanium in the sediment. Because the rain rate of marine calcite varies far less than the rate of delivery of soil debris, color changes primarily reflect the changes in river runoff and, hence, in precipitation in the contributing river's drainage basin.

Isotopic records from well-dated cave carbonates (for example, stalagmites) complement rainfall reconstructions from continental margin sediments and afford key insights into the behavior of Earth's hydroclimate during the past climate jumps. Stalagmites form when respiration CO_2–laden soil water drips onto them. The excess CO_2 escapes into the cave air, raising the CO_3^{2-} concentration to the point where $CaCO_3$ precipitates. L. Edwards at the University of Minnesota made an important

Temperature anomaly (°C)
(2040–2050 CE minus 2006–2016 CE)

Temperature anomaly (°C)

Data min = −0.4, max = 3.5, mean = 1.1

Zonally averaged temperature anomaly (°C)
(2040–2050 CE minus 2006–2016 CE)

Fig. 5. Pattern of global warming predicted for the decade 2040 to 2050. Map shows the temperature anomaly calculated from subtracting the average temperature of the past decade (that is, CE 2006 to CE 2016) from that predicted for CE 2040 to CE 2050. By this analysis, the differential heating of the hemispheres is predicted to continue for at least the next half-century. Plots are based on results for the ensemble average of the CMIP5/IPCC RCP 8.5 modeling results (99, 100).

breakthrough when he demonstrated that stalagmite calcite could be dated with extreme accuracy based on the ratio of ^{230}Th to ^{234}U. Because growth depends on the amount of precipitation, growth can come to a halt during times of severe droughts. The duration of hiatuses produced in this way can be determined by detailed U/Th dating. In addition, the ^{18}O to ^{16}O in the stalagmite $CaCO_3$ is thought to serve as a proxy for monsoonal rainfall. The greater the monsoonal contribution, the lower the ^{18}O to ^{16}O in the cave calcite.

Three records from southern Amazonia and one from northern Amazonia (Fig. 6) indicate that a northward shift in Amazonian rainfall occurred during this transition. For example, the color of the sediment in the Cariaco Basin, north of Venezuela, underwent a sharp darkening 14.6 ky ago, documenting an increase in river runoff in northern South America (34). At the same time, the iron-to-calcium ratio of the sediment on the continental margin of the Atlantic off eastern Brazil changed in the opposite direction, documenting a major decrease in river runoff (35). A hiatus in stalagmite growth at a cave in now-dry eastern Brazil commenced close to 14.6 ky ago, confirming that a drop in rainfall over southern Amazonia occurred at that time (19). Last, a closed-basin lake in the southern portion of Bolivia's Altiplano dried up at this time. This lake, known as Tauca, was three times larger than today's Lake Titicaca 14.6 ky ago (17, 36).

Equatorial Africa
Across the Atlantic in Africa, a major increase in tropical precipitation occurred 14.6 ky ago. Cores recovered from the sediments of Lake Victoria by T. Johnson of the University of Minnesota bottom out in a terrestrial soil. Lake sediment deposited immediately above this soil affords a calendar year–converted radiocarbon age close to 14.6 ky ago (37). Thus, during the time that the thermal equator was shifted to the south, runoff from the rivers that feed Lake Victoria [in addition to other African lakes (38)], must have been far lower than now, causing the lake to go dry. Then, when the abrupt northward shift of the thermal equator took place, the rivers came back to life and filled Lake Victoria with water.

The abrupt rewetting of equatorial Africa 14.6 ky ago is reinforced by a detailed record of past hydroclimate provided by the isotopic composition of deuterium in leaf waxes from a marine core from the Gulf of Aden, just offshore of the Horn of Africa (39). Together, the evidence from these lacustrine and marine sediments suggests that there was far less rainfall in Victoria's drainage basin, and perhaps equatorial Africa as a whole, before the shift of the thermal equator 14.6 ky ago.

Western United States
Firm evidence exists that closed-basin lakes of the western United States achieved their largest extents between 16 and 15 ky ago during the Mystery Interval (40), just before the switch 14.6 ky ago. Stalagmites from caves in central and southern California (41), New Mexico (42), and Nevada (43) also record peak winter moisture during this interval. In the case of Lake Lahontan, the evidence comes from a camel bone found in a back-beach deposit associated with its highest shoreline (44). A calibrated radiocarbon age of 15.66 ± 0.13 ky was obtained on bone collagen [updated using the INTCAL13 radiocarbon calibration curve (45)]. Because camels get their carbon from terrestrial plants, there is no reservoir correction nor is there a concern about the presence of secondary radiocarbon as is the case for shoreline $CaCO_3$ tufas. The Lake Lahontan water level dropped close to its present level after 14.6 ky (46), at the same time as stalagmites throughout the southwestern United States recorded a sharp decline in winter precipitation (41–43).

Thus, 14.6 ky ago, the southward-shifted mid-latitude storm track, which is related to the position of the Pacific subtropical jet (12, 41, 47, 48), brought the moisture of northern California and Oregon to southern California and into the Great Basin (40, 46). Then, when the thermal equator moved back to the north, the delivery of this extra moisture was rerouted back to the north.

Monsoonal Asia
A major feature of Asian hydroclimate during the last deglaciation was the rapid invigoration of South Asian monsoons 14.6 ky ago. Although the most prominent feature of the oxygen isotope records in stalagmites is a 20-ky cycle (49), which closely tracks the variation of boreal summer insolation related to Earth's precession cycle (see Fig. 7) (50–53), superimposed upon this cycle are abrupt millennial changes in monsoon strength that align with temperature swings registered in the Greenland ice cores. The sense of the orbital cycles in both hemispheres is that the stronger the summer insolation, the more depleted is the heavy isotope—consistent with stronger monsoons. An insolation driver of the Asian monsoon makes sense because monsoons are, in general, related to seasonal heating of the land (53, 54). Here, our interest lies in the millennial variations that punctuate the 20-ky insolation cycles.

All of the temperature jumps recorded in Greenland ice are mirrored in China's stalagmite record (52, 55). The Asian monsoons strengthened during interstadials and weakened during stadials (53). This pattern is also observed in the reflectance of sediments deposited in the Arabian Sea, offshore of the Indus River mouth (56). Abrupt changes in the Indian Monsoon runoff, as recorded in the Arabian Sea, took place in concert with the isotopic shifts registered in Greenland ice and Chinese stalagmites. In particular, the warming spike 14.6 ky ago that was registered in Greenland ice was accompanied by a strengthening of the South Asian monsoons, as recorded in Chinese stalagmites (50, 51) and the Indus River fan sediments in the Arabian Sea (56).

Antarctic ice core insights into Northern Hemisphere monsoons
One other record merits mention. Whereas stalagmite δ^{18}O records are interpreted to reflect the strength of specific monsoonal systems, the ^{18}O-to-^{16}O ratio for atmospheric O_2 trapped in ice core air bubbles provides clues into the past behavior of the Northern Hemisphere monsoon belt as a whole (57). The δ^{18}O of atmospheric O_2 is currently offset from that of ocean water by about 24‰. This offset is generated by the preferential incorporation of isotopically light O_2 (that is, $^{16}O^{16}O$) during respiration. Modulating this offset is the isotopic composition of rainfall. As shown in Fig. 8, precise and detailed oxygen isotope measurements on the O_2 stored in Antarctic ice reveal that the signature of the isotopic composition of the O_2 being added to the atmosphere is very similar to that exhibited by the Chinese stalagmites (57). The amplitudes of the millennial-scale changes are about one quarter of those in the Hulu Cave stalagmite δ^{18}O record (see Fig. 8). This correspondence suggests that rainfall in the entire Northern Hemisphere monsoon belt undergoes isotopic changes similar to those registered in southeast China. Of course, the isotopic changes in the Southern Hemisphere monsoons oppose those in the north (58). However, because the northern monsoonal zone is much larger than the southern one, the northern O_2 production dominates the signal.

Summary of global hydroclimatic changes ~14.6 ky ago
Consistent with the south-to-north jump of the latitude of the thermal equator, hydrological changes in the Southern Hemisphere occurred in
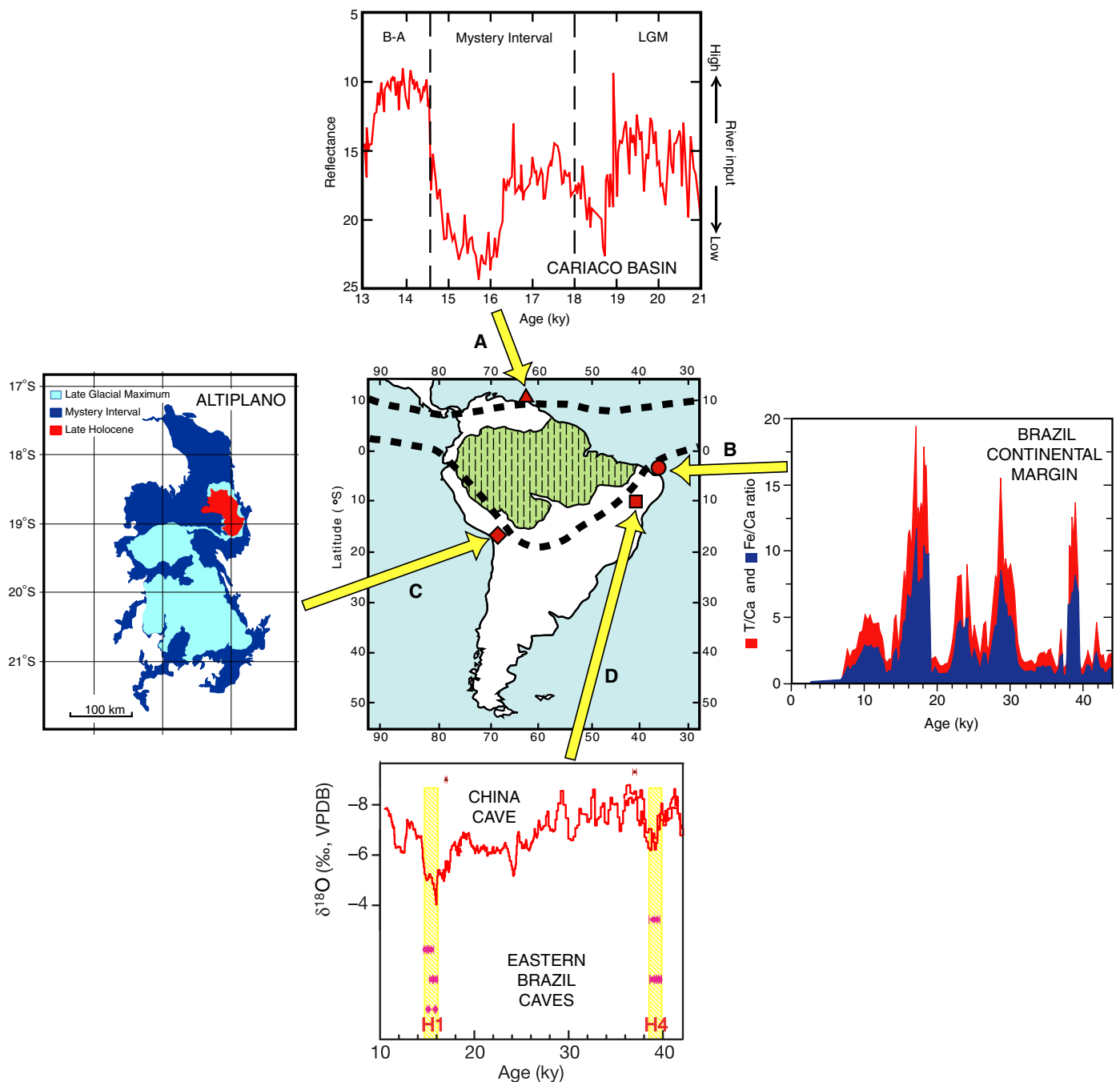
Fig. 6. Evidence in support of a northward shift in the location of the Amazonian rain belt 14.6 ky ago. (**A**) Drop in reflectance of sediments in the Cariaco Basin caused by an increase in rainfall in Venezuela (*34*). B-A, Bølling-Allerød. (**B**) A drop in the ratio of soil debris to marine calcite in a sediment core suggests a decrease in rainfall in eastern Brazil (*35*). (**C**) A lake in the southern portion of Bolivia's Altiplano three times the size of today's Titicaca dried up at about this time (*17*, *36*). (**D**) The cessation of a brief episode of stalagmite growth in eastern Brazil indicates a switch to dry conditions (*19*). It is interesting to note that at the time of this drop in Brazilian rainfall, the Chinese monsoons were becoming stronger (*51*).

antiphase with those in the Northern Hemisphere during the abrupt change 14.6 ky ago (*55*). In the Northern Hemisphere, the Cariaco Basin began to receive more terrigenous input from enhanced Venezuelan runoff, a consequence of a northward shift of the ITCZ (*34*). Chinese stalagmites recorded a switch toward more ^{18}O-depleted values, indicating an abrupt strengthening of the South Asian monsoons. Closed-basin lakes at 40°N latitude in North America dried up, possibly

in response to a northward-shifted Pacific storm track. Equatorial Africa became wetter.

At the same time in the Southern Hemisphere, stalagmites in southern Brazil recorded a switch toward more ^{18}O-enriched values, signifying a decrease in southern Amazonian tropical rainfall 14.6 ky ago (*19*). The level of paleolake Tauca dropped as the ITCZ shifted to the north (Fig. 6) (*17*, *36*). Likewise, the Australian monsoon weakened, as shown
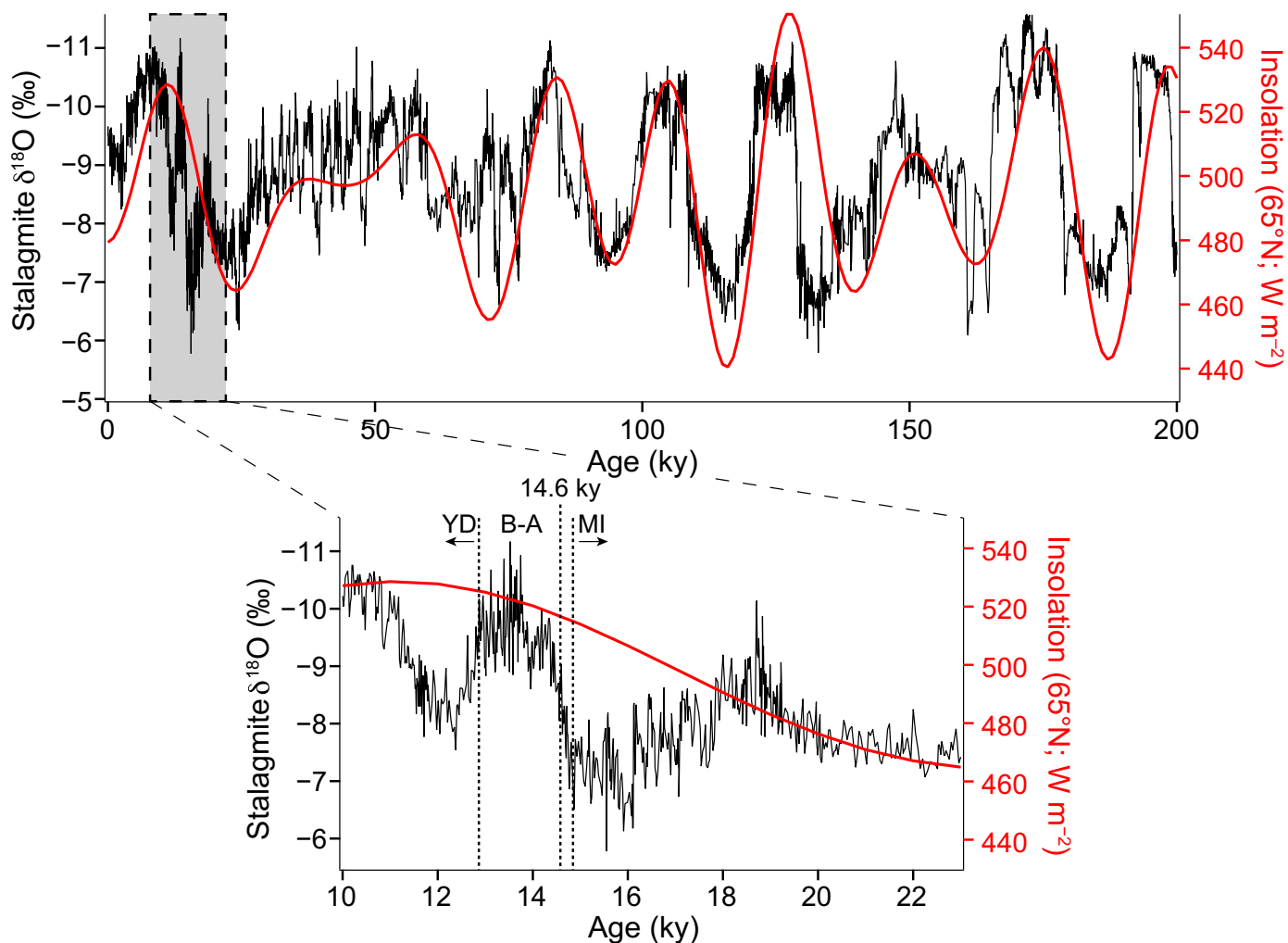
Fig. 7. Chinese Cave ^{18}O record. Composite oxygen isotope record for Chinese stalagmites for the last 200 ky (above) and for the period 10 to 18 ky ago (below) (*49*). On the long term, the record follows Northern Hemisphere summer insolation; the higher the insolation, the greater the ^{18}O deficiency. On the short term, ^{18}O follows jumps in the latitude of the thermal equator. Note that 14.7 ky ago [the beginning of the Mystery Interval (MI)], the ^{18}O-to-^{16}O ratio began a steep rise, marking a strengthening of the monsoons. YD, Younger Dryas.

by a shift toward more enriched ^{18}O values recorded in a stalagmite from a cave in Flores (10°S) (*58*). This all coincided with the onset of the Antarctic Cold Reversal in the Southern Hemisphere, which involved an equatorward shift of the Subtropical Front and the austral westerlies, sea-ice expansion, and overall cooling in the Southern Hemisphere middle and high latitudes (*31*).

The bottom line is that this shift in the latitude of the thermal equator 14.6 ky ago perturbed rainfall patterns over the entire planet, as illustrated in Fig. 9. We argue that the same thing will happen because anthropogenic CO_2 preferentially heats the Northern Hemisphere with respect to the Southern Hemisphere.

THE LITTLE ICE AGE SHIFT

Is it appropriate to assume that the hydroclimate dynamics of the last glacial termination apply to the interglacial climate of today? Here, we argue that shifts of the thermal equator, albeit smaller in magnitude, have also occurred in the more recent past. For example, there is evidence to suggest that a southward shift of the thermal equator may also

have occurred during the more recent Little Ice Age (LIA) cold period (ca. CE 1200 to CE 1850), when Earth's climatic boundary conditions were more like those of today (for example, same sea level, same ice cover, same ocean circulation). This Northern Hemispheric cooling (~1°C colder than today in the boreal summer) is well recorded by Northern Hemisphere mountain glaciers (*59–69*) and by thermal profiles in Greenland ice (*70*). It was about $1/6$ (in the south) to $1/10$ (in the north) of the cooling experienced during the LGM.

An important piece of evidence for a southward shift of the thermal equator during the LIA comes from the records kept in the sediments of lakes on a north-south trending chain of small islands in the central equatorial Pacific (*71*). Lakes on islands situated beneath the Pacific's narrow rain belt overflow to the sea. These lakes have sediments akin to those expected in well-flushed water bodies. However, lakes on islands outside the rain belt where evaporation exceeds precipitation do not overflow. Sediments of these lakes consist of bacterial mats. A series of sediment cores from these islands suggest that during the LIA, the rain belt was displaced ~800 km south of its current position (*71*).
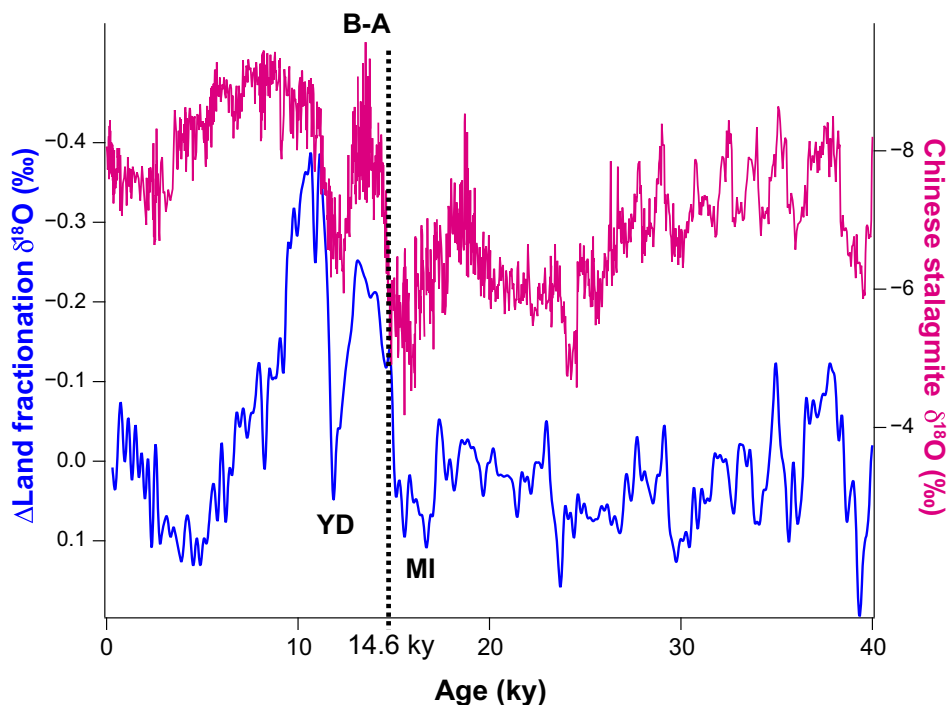
**Fig. 8. Atmospheric ^{18}O of O_2 record.** Shown in blue is the deconvolved record of the oxygen isotope composition of the O_2 contained in polar ice, also considered the change in land fractionation (57). This deconvolution takes into account the residence time of O_2 in the atmosphere (~1000 years). This reconstruction of the globally averaged isotopic composition of O_2 is markedly similar to that for Chinese stalagmites shown above in purple [a composite record compiled from multiple caves (49, 51, 101)].
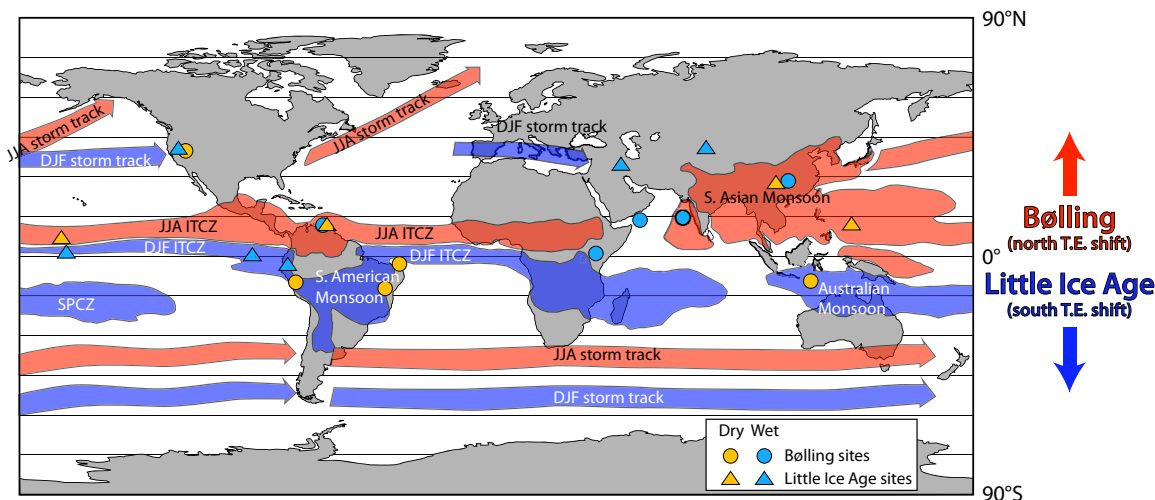
Fig. 9. Schematic map depicting seasonal shift of tropical rain belts and mid-latitude storm tracks. Evidence from the paleoclimate record teaches us that these rain belts shifted toward the north during the Bølling warming, in which the Northern Hemisphere warmed faster than the Southern Hemisphere, and to the south during the LIA, when the Northern Hemisphere experienced a greater magnitude of cooling than the Southern Hemisphere. Red, JJA rainfall; blue, DJF rainfall. Sites discussed in the text are plotted as blue-filled (wet) and tan-filled (dry) circles (Bølling) and triangles (LIA). SPCZ, South Pacific convergence zone; T.E., thermal equator.

Additional support for this southward shift comes from the comparison of oxygen isotope records kept in Chinese stalagmites, as well as lake sediments and ice cores from the tropical Andes of South America (Fig. 10). For example, oxygen isotope signatures from Chinese stalagmites and Peruvian lacustrine carbonates are mirror images of one another. The stalagmite from China shows a LIA bulge toward more positive values (that is, weaker monsoons), whereas the oxygen isotope curve based on lacustrine sediments from Peru shows a similar bulge but toward more negative values (that is, stronger monsoons). A similar pattern emerges when comparing the record of continental runoff off the northern coast of Venezuela, as recorded by the percent Ti in sediments in the Cariaco Basin (72), with snowfall accumulation rates determined from an ice core taken from the Quelccaya Ice Cap in the Peruvian Andes (73). Runoff subsided in Venezuela, and precipitation increased in Peru during the LIA, consistent with a southward shift of the ITCZ and strengthening of the South American monsoon.
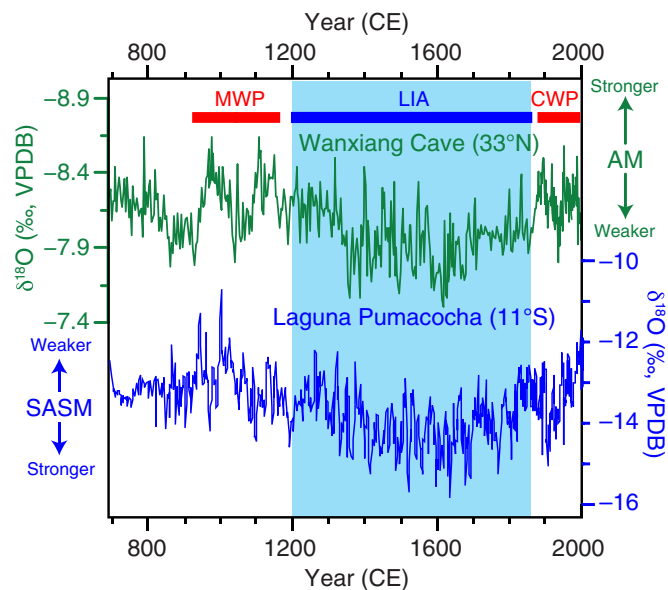
Fig. 10. LIA isotopic records for the past 1300 years from Chinese stalagmites [33°N (102)] and from Peruvian lacustrine carbonate sediments [11°S (103, 104)]. Note that the scales are in the opposite sense (that is, more negative is up for China and down for Peru). During the LIA, ¹⁸O ratios recorded in China became less negative and those in Peru became more negative. This is consistent with a southward shift in the latitude of the thermal equator. The figure is adapted with permissions from Broecker and Putnam (33). VPDB, Vienna Pee Dee belemnite; AM, Australian monsoon; SASM, South Asian summer monsoon.

In the Northern Hemisphere middle latitudes, arid regions became wetter during the LIA. For example, river runoff in the eastern Sierra Nevada increased and closed-basin lakes in the American southwest rose toward their most recent highstands (74, 75). In addition, runoff in the interior Asian deserts (61) and the Middle East (76, 77) increased. Wetting of northern mid-latitude drylands may have been related to a strengthening and/or southward shift of the boreal westerlies that attended the southward shift of the ITCZ during the LIA.

Evidence for LIA temperature change in the Southern Hemisphere is less clear. However, evidence from Southern Hemisphere mountain glaciers suggests that glacial advances that occurred during LIA time were of a smaller magnitude than those in the north (59, 78–80). Thermal records in Antarctic ice suggest that a mean annual cooling occurred but that it was smaller than that recorded in Greenland (81), implying a net "flattening" of the interhemispheric temperature contrast. Recent precipitation reconstructions based on lacustrine bio-markers from the Galápagos Islands further support the case for a southward shift of the ITCZ during the LIA (82, 83).

There is no consensus regarding what caused the LIA. The most popular scenario involves a combination of more frequent volcanic eruptions and weaker solar output. However, reconstructions of previous solar luminosity are highly uncertain. In addition, although volcanic eruptions during that time period are well documented, the impact of eruptions on incoming solar radiation is not. Another possibility is that during this time period, the ocean was taking up heat. Evidence exists that there was a 10 to 15% decrease in the production of deep water in the northern Atlantic (84), inferred from a reconstruction of the tilt of isopycnal horizons across the Florida Straits. Although causes and consequences of the LIA remain uncertain, it appears that the Northern

Hemisphere cooled more than the Southern Hemisphere, thereby causing the thermal equator to shift to the south and, in turn, Earth's rain belts. We note that evidence is conflicting with regard to whether the rain belts shifted south during the LIA (33, 71, 85) or whether the hydroclimatic response to the LIA was a more complex mosaic of regional changes [for example, the work of Yan et al. (86)]. It is important that LIA hydroclimatic changes be better documented so that, if indeed a southward shift in the thermal equator did occur, then the validity of applying this concept to future greenhouse warming can be correspondingly strengthened.

THE ROLE OF SEASONALITY

Although the mean-annual temperature of the planet has warmed by about 1°C over the past century, this warming has been neither spatially nor seasonally uniform. In addition to the observation that the Northern Hemisphere has warmed about twice as much as the Southern Hemisphere since the CE 1950s, we show in Fig. 11 that most of this interhemispheric temperature contrast has developed during the months of December, January, and February (that is, boreal winter/austral summer). In contrast, the rate of interhemispheric heating during the months of June, July, and August (that is, boreal summer/austral winter) has been more uniform, with about a degree of warming (on average) registered in both hemispheres since the CE 1950s. Thus, we consider that rainfall patterns that develop during boreal summer might respond in the sense predicted by Held and Soden (1), with tropical focusing of rainfall in the Northern Hemisphere monsoon regions and further aridification of the mid-latitude drylands. On the other hand, rainfall patterns developing during boreal winter may be influenced by the addition of a northward shift of Earth's thermal equator. Another way of looking at this is that the thermal equator will move progressively less far toward the south with each ensuing northern winter. Specific hydrological impacts may include:

1) A northward shift of the Pacific subtropical jet during the boreal winter, which will have the effect of "steering" moisture north and away from Sierra Nevada and the Great Basin of western North America (12, 47, 48), further depleting winter snowpacks that supply water for the inhabitants of the southwestern United States (16, 87, 88).

2) A weakening of the Australian and South American monsoon systems, which develop during austral summer.

3) A general northward shift of the winter jet over the North Atlantic, steering moisture north and away from the Mediterranean region, diminishing precipitation in the Middle East (89).

4) A decrease in the seasonal latitudinal range of the ITCZ, resulting in the ITCZ extending less far south with each boreal winter.
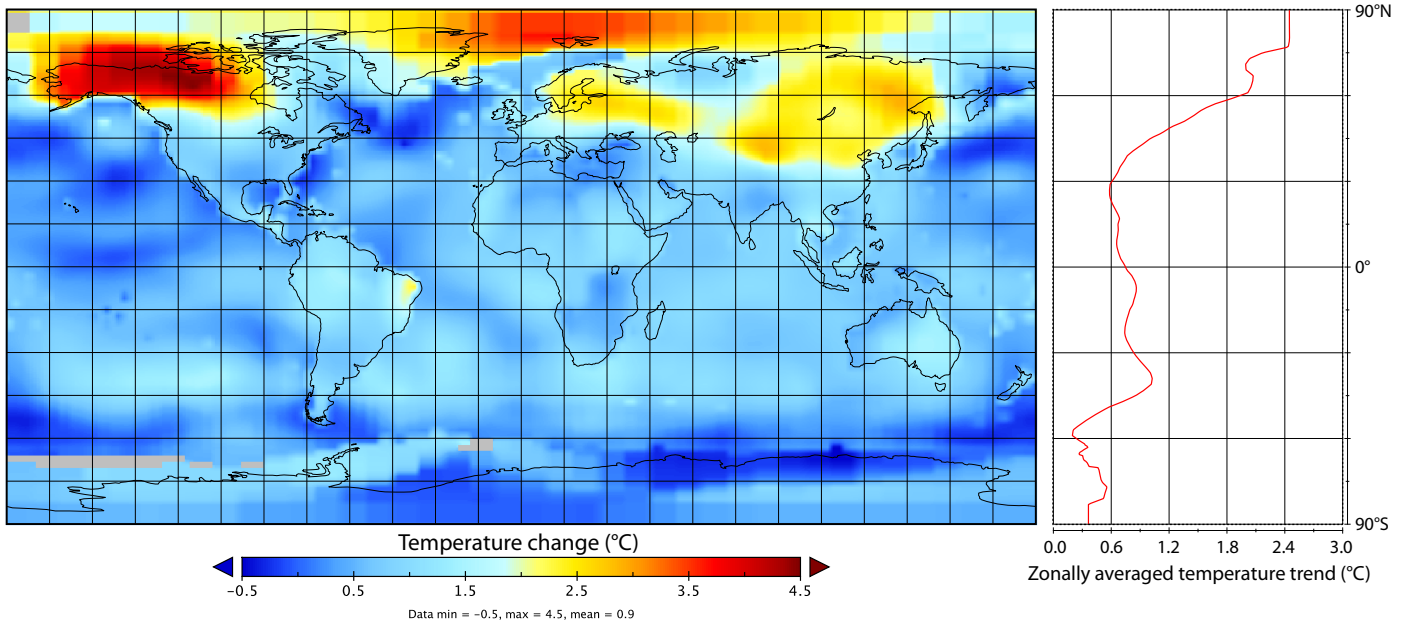
FUTURE PROGNOSIS

If both tropical focusing of rainfall and a northward shift of tropical/mid-latitude rain belts were to accompany the ongoing CO₂ warming as we suggest, then the following predictions can be made:
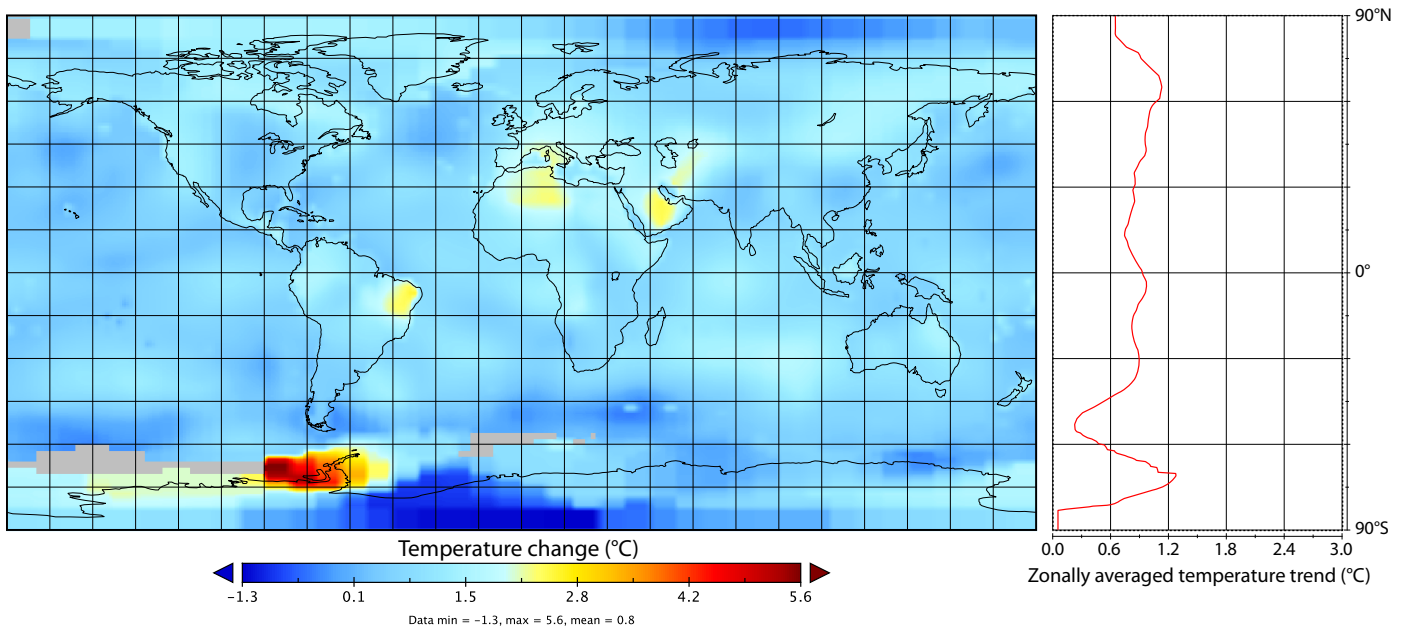
1) The tropics will become wetter, and the subtropics and middle latitudes will become drier. This will be most noticeable in June, July, and August. During these months, the interhemispheric temperature gradient has not changed much over the past several decades.

2) Northern Hemisphere monsoon rainfall will intensify and that in the Southern Hemisphere will weaken. The intensification of Northern Hemisphere monsoon systems, which develop in the boreal summer, might be in response to the tropical focusing of the hydrological system under a warming world, as suggested by Held and Soden (1). The weakening of

Global seasonal temperature trends (°C)
(over period from 1951 to 2015 CE)

A Dec-Jan-Feb

Temperature change (°C)

−0.5   0.5   1.5   2.5   3.5   4.5

Data min = −0.5, max = 4.5, mean = 0.9

Zonally averaged temperature trend (°C)

0.0   0.6   1.2   1.8   2.4   3.0

B June-July-Aug

Temperature change (°C)

−1.3   0.1   1.5   2.8   4.2   5.6

Data min = −1.3, max = 5.6, mean = 0.8

Zonally averaged temperature trend (°C)

0.0   0.6   1.2   1.8   2.4   3.0

Fig. 11. The seasonal expression of global warming trends since CE 1951. Gridded temperature trends (left) and zonally averaged temperature trends (right) for the boreal winter (December-January-February) (**A**) and summer (June-July-August) (**B**) seasons, calculated for the period spanning CE 1951 to CE 2015. Plots are based on GISTEMP Reanalysis data set (*96*, *97*). The interhemispheric temperature contrast appears to be a December-January-February phenomenon.

Southern Hemisphere monsoons might occur as a consequence of a northward shift of the thermal equator during boreal winter months.

3) The drylands of the western United States, inner Asia, and the Middle East will become even drier.

4) Amazonia will shift to the north, making Venezuela wetter and eastern Brazil and the Bolivian Altiplano drier.

CAVEATS
With regard to future predictions, several caveats must be kept in mind:

1) Instead of being the consequence of differential hemispheric heating by reduction of wintertime boreal sea ice, it will be the result of differential hemispheric warming of land relative to sea (although diminution of Arctic sea ice will no doubt play a role).

2) It is possible that the ITCZ could shift northward even with uniform heating of the polar hemispheres. This would be due to an increase in the cross-equatorial energy transport that is expected for a warming world (90).

3) During the intervals when the northern Atlantic was covered with ice, there was more dust in the northern atmosphere reinforcing the hemispheric temperature contrast. Currently, the presence of anthropogenic sulfate in the northern atmosphere counters the CO_2 warming.

4) Likewise, tropical precipitation in general, and the South Asian monsoon system in particular, has not strengthened as predicted (91–93). Anthropogenic aerosols may be suppressing the development of Asian monsoons by blocking incoming solar radiation from heating the Indian land surface (91, 94). A potentially positive outcome of reducing air pollution would be a strengthening of the South Asian summer monsoon.

5) The reorganization of the ocean's thermohaline circulation that accompanied each of the glacial shifts in the thermal equator is less likely to play a role as CO_2 warms the world.

6) Influences of large Northern Hemisphere ice sheets and of land exposed by lower sea level, which may have played some role in the hydroclimatic changes that occurred during the last deglaciation, will be absent in future scenarios.

CONCLUSIONS

Model-based simulations of the ongoing rise in atmospheric CO_2 predict that the Northern Hemisphere will warm faster than the Southern Hemisphere. The interhemispheric temperature difference created in this way will increase with time until the rate of CO_2 rise levels off and ocean heating catches up with that for the atmosphere. The world's rain belts, at least during the December-January-February months, will shift in concert with the interhemispheric temperature difference. Then, as CO_2 concentrations start to decrease, either because they are being taken up by the ocean or purposefully captured and buried, the rain belts will shift back to the south, at least during the boreal winter season.

The magnitude of the shift in precipitation belts at the peak of the anthropogenic warming may be closer to that 14.6 ky ago than that for the LIA. The high latitudes of the Northern Hemisphere may heat up by as much as ~3°C more than in the Southern Hemisphere by CE 2050 with continued CO_2 rise. Superimposed upon impacts of the shifting thermal equator, registered most strongly in the boreal winter season, will be the intensification of tropical rainfall at the expense of rainfall in the subtropics and middle latitudes, which may be expressed most prominently during boreal summer. This will have a similar time trend following global temperature rather than the interhemispheric temperature contrast.

REFERENCES AND NOTES

1. I. M. Held, B. J. Soden, Robust responses of the hydrological cycle to global warming. *J. Climate* **19**, 5686–5699 (2006).
2. J. C. H. Chiang, A. R. Friedman, Tropical cooling, interhemispheric thermal gradients, and tropical climate change. *Annu. Rev. Earth Planet. Sci.* **40**, 383–412 (2012).
3. A. R. Friedman, Y.-T. Hwang, J. C. H. Chiang, D. M. W. Frierson, Interhemispheric temperature asymmetry over the twentieth century and future projections. *J. Climate* **26**, 5419–5433 (2013).
4. T. Schneider, T. Bischoff, G. H. Haug, Migrations and dynamics of the intertropical convergence zone. *Nature* **513**, 45–53 (2014).
5. P. U. Clark, A. C. Mix, Ice sheets and sea level of the Last Glacial Maximum. *Quat. Sci. Rev.* **21**, 1–7 (2002).
6. L. V. Benson, S. P. Lund, J. W. Burdett, M. Kashgarian, T. P. Rose, J. P. Smoot, M. Schwartz, Correlation of late-Pleistocene lake-level oscillations in Mono Lake, California, with North Atlantic climate events. *Quatern. Res.* **49**, 1–10 (1998).
7. D. R. Currey, C. G. Oviatt, "Durations, average rates, and probable causes of Lake Bonneville expansions, stillstand, and contractions during the last deep-lake cycle, 32,000 to 10, 000 years ago," in *Problems and the Prospects for Predicting Great Salt Lake Levels*, P. A. Kay, H. F. Diaz, Eds. (Central Public Affairs Administration, University of Utah, 1985), pp. 9–24.
8. W. Broecker, Long-term water prospects in the Western United States. *J. Climate* **23**, 6669–6683 (2010).
9. A. Schramm, M. Stein, S. L. Goldstein, Calibration of the ^{14}C time scale to >40 ka by ^{234}U–^{230}Th dating of Lake Lisan sediments (last glacial Dead Sea). *Earth Planet. Sci. Lett.* **175**, 27–40 (2000).
10. A. Cartwright, J. Quade, S. Stine, K. D. Adams, W. Broecker, H. Cheng, Chronostratigraphy and lake-level changes of Laguna Cari-Laufquén, Río Negro, Argentina. *Quatern. Res.* **76**, 430–440 (2011).
11. J. Quade, W. S. Broecker, Dryland hydrology in a warmer world: Lessons from the Last Glacial period. *Eur. Phys. J. Spec. Top.* **176**, 21–36 (2009).
12. A. E. Putnam, Palaeoclimate: A glacial zephyr. *Nat. Geosci.* **8**, 175–176 (2015).
13. A. E. Putnam, J. M. Schaefer, G. H. Denton, D. J. A. Barrell, S. D. Birkel, B. G. Andersen, M. R. Kaplan, R. C. Finkel, R. Schwartz, The Last Glacial Maximum at 44°S documented by a ^{10}Be moraine chronology at Lake Ohau, Southern Alps of New Zealand. *Quat. Sci. Rev.* **62**, 114–141 (2013).
14. M. I. Budyko, *The Heat Balance of the Earth's Surface* (U.S. Department of Commerce, 1958).
15. R. D. Koster, B. M. Fekete, G. J. Huffman, P. W. Stackhouse Jr., Revisiting a hydrological analysis framework with International Satellite Land Surface Climatology Project Initiative 2 rainfall, net radiation, and runoff fields. *J. Geophys. Res.* **111**, D22S05 (2006).
16. B. J. Hatchett, D. P. Boyle, A. E. Putnam, S. D. Bassett, Placing the 2012–2015 California-Nevada drought into a paleoclimatic context: Insights from Walker Lake, California-Nevada, USA. *Geophys. Res. Lett.* **42**, 8632–8640 (2015).
17. P.-H. Blard, F. Sylvestre, A. K. Tripati, C. Claude, C. Causse, A. Coudrain, T. Condom, J.-L. Seidel, F. Vimeux, C. Moreau, J.-P. Dumoulin, J. Lavé, Lake highstands on the Altiplano (Tropical Andes) contemporaneous with Heinrich 1 and the Younger Dryas: New insights from ^{14}C, U–Th dating and δ^{18}O of carbonates. *Quat. Sci. Rev.* **30**, 3973–3989 (2011).
18. J. C. H. Chiang, C. M. Bitz, Influence of high latitude ice cover on the marine Intertropical Convergence Zone. *Climate Dynam.* **25**, 477–496 (2005).
19. X. Wang, A. S. Auler, R. L. Edwards, H. Cheng, P. S. Cristalli, P. L. Smart, D. A. Richards, C.-C. Shen, Wet periods in northeastern Brazil over the past 210 kyr linked to distant climate anomalies. *Nature* **432**, 740–743 (2004).
20. J. L. Russell, K. W. Dixon, A. Gnanadesikan, R. J. Stouffer, J. R. Toggweiler, The Southern Hemisphere westerlies in a warming world: Propping open the door to the deep ocean. *J. Climate* **19**, 6382–6390 (2006).
21. J. P. Severinghaus, E. J. Brook, Abrupt climate change at the end of the last glacial period inferred from trapped air in polar ice. *Science* **286**, 930–934 (1999).
22. G. H. Denton, R. B. Alley, G. C. Comer, W. S. Broecker, The role of seasonality in abrupt climate change. *Quat. Sci. Rev.* **24**, 1159–1182 (2005).
23. C. Buizert, V. Gkinis, J. P. Severinghaus, F. He, B. S. Lecavalier, P. Kindler, M. Leuenberger, A. E. Carlson, B. Vinther, V. Masson-Delmotte, J. W. C. White, Z. Liu, B. Otto-Bliesner, E. J. Brook, Greenland temperature response to climate forcing during the last deglaciation. *Science* **345**, 1177–1180 (2014).
24. G. Denton, W. S. Broecker, R. B. Alley, The mystery interval 17.5 to 14.5 kyrs ago. *PAGES News* **14**, 14–16 (2006).
25. S. Barker, P. Diz, M. J. Vautravers, J. Pike, G. Knorr, I. R. Hall, W. S. Broecker, Interhemispheric Atlantic seesaw response during the last deglaciation. *Nature* **457**, 1097–1102 (2009).
26. E. Bard, F. Rostek, J.-L. Turon, S. Gendreau, Hydrological impact of Heinrich events in the subtropical northeast Atlantic. *Science* **289**, 1321–1324 (2000).
27. J. F. McManus, R. Francois, J.-M. Gherardi, L. D. Keigwin, S. Brown-Leger, Collapse and rapid resumption of Atlantic meridional circulation linked to deglacial climate changes. *Nature* **428**, 834–837 (2004).
28. H. Renssen, P. W. Bogaart, Atmospheric variability over the ~14.7 kyr BP stadial-interstadial transition in the North Atlantic region as simulated by an AGCM. *Climate Dynam.* **20**, 301–313 (2003).
29. W. S. Broecker, Abrupt climate change revisited. *Global Planet. Change* **54**, 211–215 (2006).
30. R. F. Anderson, S. Ali, L. I. Bradtmiller, S. H. Nielsen, M. Q. Fleisher, B. E. Anderson, L. H. Burckle, Wind-driven upwelling in the Southern Ocean and the deglacial rise in atmospheric CO_2. *Science* **323**, 1443–1448 (2009).
31. A. E. Putnam, G. H. Denton, J. M. Schaefer, D. J. A. Barrell, B. G. Andersen, R. C. Finkel, R. Schwartz, A. M. Doughty, M. R. Kaplan, C. Schlüchter, Glacier advance in southern middle latitudes during the Antarctic Cold Reversal. *Nat. Geosci.* **3**, 700–704 (2010).
32. G. H. Denton, R. F. Anderson, J. R. Toggweiler, R. L. Edwards, J. M. Schaefer, A. E. Putnam, The last glacial termination. *Science* **328**, 1652–1656 (2010).

33. W. S. Broecker, A. E. Putnam, Hydrologic impacts of past shifts of Earth's thermal equator offer insight into those to be produced by fossil fuel CO_2. *Proc. Natl. Acad. Sci. U.S.A.* **110**, 16710–16715 (2013).

34. L. C. Peterson, G. H. Haug, K. A. Hughen, U. Röhl, Rapid changes in the hydrologic cycle of the tropical Atlantic during the last glacial. *Science* **290**, 1947–1951 (2000).

35. H. W. Arz, J. Pätzold, G. Wefer, Correlated millennial-scale changes in surface hydrography and terrigenous sediment yield inferred from last-glacial marine deposits off northeastern Brazil. *Quatern. Res.* **50**, 157–166 (1998).

36. C. Placzek, J. Quade, P. J. Patchett, Geochronology and stratigraphy of late Pleistocene lake cycles on the southern Bolivian Altiplano: Implications for causes of tropical climate change. *Geol. Soc. Am. Bull.* **118**, 515–532 (2006).

37. T. C. Johnson, C. A. Scholz, M. R. Talbot, K. Kelts, R. D. Ricketts, G. Ngobi, K. Beuning, I. Ssemmanda, J. W. McGill, Late Pleistocene desiccation of Lake Victoria and rapid evolution of cichlid fishes. *Science* **273**, 1091–1093 (1996).

38. J. C. Stager, D. B. Ryves, B. M. Chase, F. S. R. Pausata, Catastrophic drought in the Afro-Asian monsoon region during Heinrich event 1. *Science* **331**, 1299–1302 (2011).

39. J. E. Tierney, P. B. deMenocal, Abrupt shifts in horn of Africa hydroclimate since the last glacial maximum. *Science* **342**, 843–846 (2013).

40. J. S. Munroe, B. J. C. Laabs, Temporal correspondence between pluvial lake highstands in the southwestern US and Heinrich Stadial 1. *J. Quaternary Sci.* **28**, 49–58 (2013).

41. J. L. Oster, I. P. Montañez, L. R. Santare, W. D. Sharp, C. Wong, K. M. Cooper, Stalagmite records of hydroclimate in central California during termination 1. *Quat. Sci. Rev.* **127**, 199–214 (2015).

42. Y. Asmerom, V. J. Polyak, S. J. Burns, Variable winter moisture in the southwestern United States linked to rapid glacial climate shifts. *Nat. Geosci.* **3**, 114–117 (2010).

43. M. S. Lachniet, R. F. Denniston, Y. Asmerom, V. J. Polyak, Orbital control of western North America atmospheric circulation and climate over two glacial cycles. *Nat. Commun.* **5**, 3805 (2014).

44. K. D. Adams, S. G. Wesnousky, Shoreline processes and the age of the Lake Lahontan highstand in the Jessup embayment, Nevada. *Geol. Soc. Am. Bull.* **110**, 1318–1332 (1998).

45. P. J. Reimer, E. Bard, A. Bayliss, J. W. Beck, P. G. Blackwell, C. B. Ramsey, C. E. Buck, H. Cheng, R. L. Edwards, M. Friedrich, P. M. Grootes, T. P. Guilderson, H. Haflidason, I. Hajdas, C. Hatté, T. J. Heaton, D. L. Hoffmann, A. G. Hogg, K. A. Hughen, K. F. Kaiser, B. Kromer, S. W. Manning, M. Niu, R. W. Reimer, D. A. Richards, E. M. Scott, J. R. Southon, R. A. Staff, C. S. M. Turney, J. van der Plicht, IntCal13 and Marine13 radiocarbon age calibration curves 0–50,000 years cal BP. *Radiocarbon* **55**, 1869–1887 (2013).

46. W. S. Broecker, D. McGee, K. D. Adams, H. Cheng, R. Lawrence Edwards, C. G. Oviatt, J. Quadee, A Great Basin-wide dry episode during the first half of the Mystery Interval? *Quat. Sci. Rev.* **28**, 2557–2563 (2009).

47. J. C. H. Chiang, S.-Y. Lee, A. E. Putnam, X. Wang, South Pacific Split Jet, ITCZ shifts, and atmospheric North–South linkages during abrupt climate changes of the last glacial period. *Earth Planet. Sci. Lett.* **406**, 233–246 (2014).

48. J. L. Oster, D. E. Ibarra, M. J. Winnick, K. Maher, Steering of westerly storms over western North America at the Last Glacial Maximum. *Nat. Geosci.* **8**, 201–205 (2015).

49. H. Cheng, R. L. Edwards, A. Sinha, C. Spötl, L. Yi, S. Chen, M. Kelly, G. Kathayat, X. Wang, X. Li, X. Kong, Y. Wang, Y. Ning, H. Zhang, The Asian monsoon over the past 640,000 years and ice age terminations. *Nature* **534**, 640–646 (2016).

50. H. Cheng, R. L. Edwards, W. S. Broecker, G. H. Denton, X. Kong, Y. Wang, R. Zhang, X. Wang, Ice age terminations. *Science* **326**, 248–252 (2009).

51. Y. J. Wang, H. Cheng, R. L. Edwards, Z. S. An, J. Y. Wu, C.-C. Shen, J. A. Dorale, A high-resolution absolute-dated Late Pleistocene monsoon record from Hulu Cave, China. *Science* **294**, 2345–2348 (2001).

52. Y. Wang, H. Cheng, R. L. Edwards, X. Kong, X. Shao, S. Chen, J. Wu, X. Jiang, X. Wang, Z. An, Millennial- and orbital-scale changes in the East Asian monsoon over the past 224,000 years. *Nature* **451**, 1090–1093 (2008).

53. Z. An, W. Guoxiong, L. Jianping, S. Youbin, L. Yimin, Z. Weijian, C. Yanjun, D. Anmin, L. Li, M. Jiangyu, S. Hai, S. Zhengguo, T. Liangcheng, Y. Hong, A. Hong, C. Hong, F. Juan, Global monsoon dynamics and climate change. *Annu. Rev. Earth Planet. Sci.* **43**, 29–77 (2015).

54. Y. Goldsmith, W. S. Broecker, H. Xu, P. J. Polissar, P. B. deMenocal, N. Porat, J. Lan, P. Cheng, W. Zhou, Z. An, Northward extent of East Asian monsoon covaries with intensity on orbital and millennial timescales. *Proc. Natl. Acad. Sci. U.S.A.* **114**, 1817–1821 (2017).

55. X. Wang, A. S. Auler, R. L. Edwards, H. Cheng, E. Ito, M. Solheid, Interhemispheric anti-phasing of rainfall during the last glacial period. *Quat. Sci. Rev.* **25**, 3391–3403 (2006).

56. G. Deplazes, A. Lückge, J.-B. W. Stuut, J. Pätzold, H. Kuhlmann, D. Husson, M. Fant, G. H. Haug, Weakening and strengthening of the Indian monsoon during Heinrich events and Dansgaard-Oeschger oscillations. *Paleoceanography* **29**, 99–114 (2014).

57. J. P. Severinghaus, R. Beaudette, M. A. Headly, K. Taylor, E. J. Brook, Oxygen-18 of O_2 records the impact of abrupt climate change on the terrestrial biosphere. *Science* **324**, 1431–1434 (2009).

58. L. K. Ayliffe, M. K. Gagan, J.-x. Zhao, R. N. Drysdale, J. C. Hellstrom, W. S. Hantoro, M. L. Griffiths, H. Scott-Gagan, E. St Pierre, J. A. Cowley, B. W. Suwargadi, Rapid interhemispheric climate links via the Australasian monsoon sensitivity to millennial climate change during the last deglaciation. *Nat. Commun.* **4**, 2908 (2013).

59. G. H. Denton, W. S. Broecker, Wobbly ocean conveyor circulation during the Holocene? *Quat. Sci. Rev.* **27**, 1939–1950 (2008).

60. J. M. Grove, The initiation of the "Little Ice Age" in regions round the North Atlantic. *Clim. Change* **48**, 53–82 (2001).

61. A. E. Putnam, D. E. Putnam, L. Andreu-Hayles, E. R. Cook, J. G. Palmer, E. H. Clark, C. Wang, F. Chen, G. H. Denton, D. P. Boyle, Little Ice Age wetting of interior Asian deserts and the rise of the Mongol Empire. *Quat. Sci. Rev.* **131**, 33–50 (2016).

62. H. Holzhauser, M. Magny, H. J. Zumbühl, Glacier and lake-level variation in west-central Europe over the last 3500 years. *Holocene* **15**, 789–801 (2005).

63. H. Holzhauser, H. J. Zumbühl, Glacier fluctuations in the western Swiss and French Alps in the 16th Century. *Clim. Change* **43**, 223–237 (1999).

64. K. Nicolussi, G. Patzelt, Discovery of early-Holocene wood and peat on the forefield on the Pasterze Glacier, Eastern Alps, Austria. *Holocene* **10**, 191–199 (2000).

65. K. Nicolussi, G. Patzelt, Untersuchungen zur holozänen Gletscherentwicklung von Pasterze und Gepatschferner (Ostalpen). *Zs. Gletscherkunde Glazialgeol.* **36**, 1–87 (2001).

66. D. J. Barclay, G. C. Wiles, P. E. Calkin, Holocene glacier fluctuations in Alaska. *Quat. Sci. Rev.* **28**, 2034–2048 (2009).

67. B. H. Luckman, The Little Ice Age in the Canadian Rockies. *Geomorphology* **32**, 357–384 (2000).

68. O. N. Solomina, R. S. Bradley, V. Jomelli, A. Geirsdottir, D. S. Kaufman, J. Koch, N. P. McKay, M. Masiokas, G. Miller, A. Nesje, K. Nicolussi, L. A. Owen, A. E. Putnam, H. Wanner, G. Wiles, B. Yang, Glacier fluctuations during the past 2000 years. *Quat. Sci. Rev.* **149**, 61–90 (2016).

69. M. Le Roy, K. Nicolussi, P. Deline, L. Astrade, J.-L. Edouard, C. Miramont, F. Arnaud, Calendar-dated glacier variations in the western European Alps during the Neoglacial: The Mer de Glace record, Mont Blanc massif. *Quat. Sci. Rev.* **108**, 1–22 (2015).

70. D. Dahl-Jensen, K. Mosegaard, N. Gundestrup, G. D. Clow, S. J. Johnsen, A. W. Hansen, N. Balling, Past temperatures directly from the Greenland Ice sheet. *Science* **282**, 268–271 (1998).

71. J. P. Sachs, D. Sachse, R. H. Smittenberg, Z. Zhang, D. S. Battisti, S. Golubic, Southward movement of the Pacific intertropical convergence zone AD 1400–1850. *Nat. Geosci.* **2**, 519–525 (2009).

72. G. H. Haug, K. A. Hughen, D. M. Sigman, L. C. Peterson, U. Röhl, Southward migration of the intertropical convergence zone through the Holocene. *Science* **293**, 1304–1308 (2001).

73. L. G. Thompson, E. Mosley-Thompson, M. E. Davis, V. S. Zagorodnov, I. M. Howat, V. N. Mikhalenko, P.-N. Lin, Annually resolved ice core records of tropical climate variability over the past ~1800 years. *Science* **340**, 945–950 (2013).

74. S. Stine, Extreme and persistent drought in California and Patagonia during medieval time. *Nature* **369**, 546–549 (1994).

75. J. A. Kleppe, D. S. Brothers, G. M. Kent, F. Biondi, S. Jensen, N. W. Driscoll, Duration and severity of Medieval drought in the Lake Tahoe Basin. *Quat. Sci. Rev.* **30**, 3269–3279 (2011).

76. S. Haghani, S. A. G. Leroy, S. Khdir, K. Kabiri, A. N. Beni, H. A. K. Lahijani, An early 'Little Ice Age' brackish water invasion along the south coast of the Caspian Sea (sediment of Langarud wetland) and its wider impacts on environment and people. *Holocene* **26**, 3–16 (2016).

77. Y. Enzel, R. Bookman, D. Sharon, H. Gvirtzman, U. Dayan, B. Ziv, M. Stein, Late Holocene climates of the Near East deduced from Dead Sea level variations and modern regional winter rainfall. *Quatern. Res.* **60**, 263–273 (2003).

78. J. M. Schaefer, G. H. Denton, M. Kaplan, A. Putnam, R. C. Finkel, D. J. A. Barrell, B. G. Andersen, R. Schwartz, A. Mackintosh, T. Chinn, C. Schlüchter, High-frequency Holocene glacier fluctuations in New Zealand differ from the northern signature. *Science* **324**, 622–625 (2009).

79. A. E. Putnam, J. M. Schaefer, G. H. Denton, D. J. A. Barrell, R. C. Finkel, B. G. Andersen, R. Schwartz, T. J. H. Chinn, A. M. Doughty, Regional climate control of glaciers in New Zealand and Europe during the pre-industrial Holocene. *Nat. Geosci.* **5**, 627–630 (2012).

80. M. R. Kaplan, J. M. Schaefer, J. A. Strelin, G. H. Denton, R. F. Anderson, M. J. Vandergoes, R. C. Finkel, R. Schwartz, S. G. Travis, J. L. Garcia, M. A. Martini, S. H. H. Nielsen, Patagonian and southern South Atlantic view of Holocene climate. *Quat. Sci. Rev.* **141**, 112–125 (2016).

81. A. J. Orsi, B. D. Cornuelle, J. P. Severinghaus, Little Ice Age cold interval in West Antarctica: Evidence from borehole temperature at the West Antarctic Ice Sheet (WAIS) Divide. *Geophys. Res. Lett.* **39**, L09710 (2012).

82. J. N. Richey, J. P. Sachs, Precipitation changes in the western tropical Pacific over the past millennium. *Geology* **44**, 671–674 (2016).

83. D. B. Nelson, J. P. Sachs, Galápagos hydroclimate of the Common Era from paired microalgal and mangrove biomarker $^2H/^1H$ values. *Proc. Natl. Acad. Sci. U.S.A.* **113**, 3476–3481 (2016).

84. D. C. Lund, J. Lynch-Steiglitz, W. B. Curry, Gulf Stream density structure and transport during the past millennium. *Nature* **444**, 601–604 (2006).

85. F. C. Ljungqvist, P. J. Krusic, H. S. Sundqvist, E. Zorita, G. Brattström, D. Frank, Northern Hemisphere hydroclimate variability over the past twelve centuries. *Nature* **532**, 94–98 (2016).

86. H. Yan, W. Wei, W. Soon, Z. An, W. Zhou, Z. Liu, Y. Wang, R. M. Carter, Dynamics of the intertropical convergence zone over the western Pacific during the Little Ice Age. *Nat. Geosci.* **8**, 315–320 (2015).

87. B. J. Hatchett, D. P. Boyle, C. B. Garner, M. L. Kaplan, A. E. Putnam, S. D. Bassett, Magnitude and frequency of wet years under a megadrought climate in the western Great Basin, USA. *Quat. Sci. Rev.* **152**, 197–202 (2016).

88. M. Dettinger, Climate change: Impacts in the third dimension. *Nat. Geosci.* **7**, 166–167 (2014).

89. C. P. Kelley, S. Mohtadi, M. A. Cane, R. Seager, Y. Kushnir, Climate change in the Fertile Crescent and implications of the recent Syrian drought. *Proc. Natl. Acad. Sci. U.S.A.* **112**, 3241–3246 (2015).

90. T. Bischoff, T. Schneider, Energetic constraints on the position of the intertropical convergence zone. *J. Climate* **27**, 4937–4951 (2014).

91. V. Ramanathan, C. Chung, D. Kim, T. Bettge, L. Buja, J. T. Kiehl, W. M. Washington, Q. Fu, D. R. Sikka, M. Wild, Atmospheric brown clouds: Impacts on South Asian climate and hydrological cycle. *Proc. Natl. Acad. Sci. U.S.A.* **102**, 5326–5333 (2005).

92. L. D. Rotstayn, M. A. Collier, J.-J. Luo, Effects of declining aerosols on projections of zonally averaged tropical precipitation. *Environ. Res. Lett.* **10**, 044018 (2015).

93. L. D. Rotstayn, U. Lohmann, Tropical rainfall trends and the indirect aerosol effect. *J. Climate* **15**, 2103–2116 (2002).

94. M. A. Bollasina, Y. Ming, V. Ramaswamy, Anthropogenic aerosols and the weakening of the South Asian Summer Monsoon. *Science* **334**, 502–505 (2011).

95. S. Solomon, D. Qin, M. Manning, Z. Chen, M. Marquis, K. B. Averyt, M. Tignor, H. L. Mille, *IPCC Fourth Assessment Report: Climate Change 2007: Climate Change 2007: Working Group I: The Physical Science Basis* (Cambridge Univ. Press, 2007).

96. GISTEMP Team, *GISS Surface Temperature Analysis (GISTEMP)* (NASA Goddard Institute for Space Studies, 2016); http://data.giss.nasa.gov/gistemp.

97. J. Hansen, R. Ruedy, M. Sato, K. Lo, Global surface temperature change. *Rev. Geophys.* **48**, RG4004 (2010).

98. R. Hijmans, S. E. Cameron, J. L. Parra, P. G. Jones, A. Jarvis, Very high resolution interpolated climate surfaces for global land areas. *Int. J. Climatol.* **25**, 1965–1978 (2005).

99. R. H. Moss, J. A. Edmonds, K. A. Hibbard, M. R. Manning, S. K. Rose, D. P. van Vuuren, T. R. Carter, S. Emori, M. Kainuma, T. Kram, G. A. Meehl, J. F. B. Mitchell, N. Nakicenovic, K. Riahi, S. J. Smith, R. J. Stouffer, A. M. Thomson, J. P. Weyant, T. J. Wilbanks, The next generation of scenarios for climate change research and assessment. *Nature* **463**, 747–756 (2010).

100. R. H. Moss, N. Nakicenovic, B. C. O'Neill, *Towards New Scenarios for Analysis of Emissions, Climate Change, Impacts, and Response Strategies* (Intergovernmental Panel on Climate Change, 2008), 132 pp.

101. C. A. Dykoski, R. L. Edwards, H. Cheng, D. Yuan, Y. Cai, M. Zhang, Y. Lin, J. Qing, Z. An, J. Revenaugh, A high-resolution, absolute-dated Holocene and deglacial Asian monsoon record from Dongee Cave, China. *Earth Planet. Sci. Lett.* **233**, 71–86 (2005).

102. P. Z. Zhang, H. Cheng, R. L. Edwards, F. Chen, Y. Wang, X. Yang, J. Liu, M. Tan, X. Wang, J. Liu, C. An, Z. Dai, J. Zhou, D. Zhang, J. Jia, L. Jin, K. R. Johnson, A test of climate, sun, and culture relationships from an 1810-year Chinese cave record. *Science* **322**, 940–942 (2008).

103. B. W. Bird, M. B. Abbott, D. T. Rodbell, M. Vuille, Holocene tropical South American hydroclimate revealed from a decadally resolved lake sediment $\delta^{18}O$ record. *Earth Planet. Sci. Lett.* **310**, 192–202 (2011).

104. B. W. Bird, M. B. Abbott, M. Vuille, D. T. Rodbell, N. D. Stansell, M. F. Rosenmeier, A 2,300-year-long annually resolved record of the South American summer monsoon from the Peruvian Andes. *Proc. Natl. Acad. Sci. U.S.A.* **108**, 8583–8588 (2011).